An Underwater Digital Photogrammetric System For Fishery Geomatics

Rongxing Li, Chuang Tao, and Weihong Zou
Department of Geomatics Engineering, The University of Calgary
2500 University Drive, NW, Calgary, Alberta, Canada T2N 1N4
Tel: 403-220-4112, Fax: 403-284-1980
E-mail: rli@acs.ucalgary.ca, WWW: http://loihi.ensu.ucalgary.ca/

R. G. Smith and T. A. Curran
Institute of Ocean Sciences, Canadian Hydrographic Services
P.O. Box 6000, 9860 W Sasnich Road, Sidney, British Columbia, Canada V8L 4B2

KEY WORDS: Underwater photogrammetry, Digital photogrammetry, CCD camera, Calibration

ABSTRACT:

A new Underwater Digital Photogrammetric System (UDPS) has been developed at The University of Calgary and Canadian Hydrographic Services. An underwater digital CCD imaging system has been mounted on a Remotely Operated Vehicle (ROV). This system will be used for fisheries and related applications in the marine environment. In this paper, the design and the implementation of this underwater digital photogrammetric system is described. The mobile photogrammetry and digital imaging technologies are employed. An efficient system calibration scheme and an underwater photogrammetric model are presented. Recent test results are given.

1. INTRODUCTION

Exploration of the vast water body of the earth is of increasing importance for fisheries, development and management of marine oil and mineral resources, and ocean floor investigation. Collecting and analyzing underwater data is a key to the exploration. Requirements for the underwater imaging technology continue to be diversified in recent years. Advances in the imaging sensor technology, particularly those in solid-state devices, led to a trend towards diverless underwater intervention systems. Intuitively, an efficient and effective technology is required to meet the demanding needs of underwater data analysis and interpretation (Turner et al., 1992).

A research project was initiated at The University of Calgary and the Canadian Hydrographic Services (CHS) to develop a mobile underwater digital photogrammetric system for fisheries and underwater environmental surveys. The current emphasis is on fish stock assessment which involves the identification of fish species, calculation of fish size and volume, visualization and measurement of sea plants. Traditionally, most of the research on the underwater resource management depends on the analysis of sonar images. However, acoustic data are of small scales. On the other hand, video images provide the capability of direct visual interpretations. Photogrammetry is recognized as a cost-effect technology to these applications. Recent advances in underwater vehicle navigation and digital imaging make photogrammetry a feasible and practical technology for applications in underwater surveys and object measurement. The quantitative rather than qualitative analysis of underwater images can be achieved by means of digital photogrammetric processing.

This paper describes an Underwater Digital Photogrammetric System (UDPS) jointly developed by The University of Calgary and CHS. Following the introduction, the system design and its configuration are given. In section 3, a reduced central perspective model and a mathematically rigorous 3D ray tracing model are described. Section 4 presents an efficient system calibration. Experimental results and concluding remarks are given in the last two sections.

2. MOBILE UNDERWATER MAPPING

2.1 Mobility Of The Underwater System

In conventional underwater survey, underwater control is a complicated work (Leatherdale and Turner, 1991). It is difficult to select fixed and identifiable points for control. Serious problems of connections between stereo models may arise. Artificial magnetic targets and grease paint marks are used to provide sufficient feature and texture for stereoscopic measurements. With the navigation capability of the GPS, underwater mobile mapping becomes a reality in recent years. Figure 1 gives a brief view of a mobile UDPS. GPS provides accurate positions of the vessel in a dynamic or semi-dynamic mode. By means of the integration of multiple local sensors, such as acoustic systems, pressure sensors and gyrocompasses, the ROV, which is equipped with a stereo imaging system, can be positioned with respect to the vessel. After the calibration of the geometric relationship between the imaging cameras and the ROV, the stereo image sequences of underwater objects can be georeferenced in a global coordinate system. Currently, the gyrocompass and the acoustic system have not been implemented.

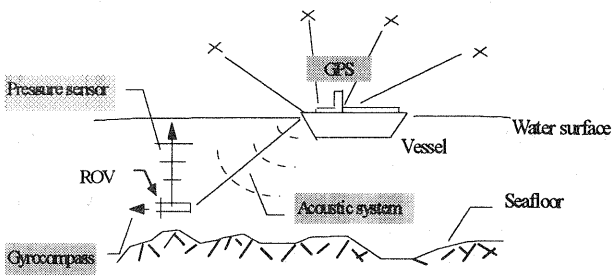

Figure 1. A mobile UDPS framework

2.2 UDPS Configuration

The system consists of four components: data acquisition, data transmission, data recording and data control (figure 2).

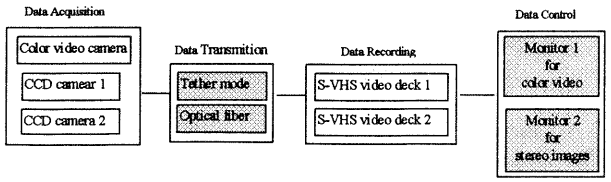

Figure 2. UDPS configuration

2.2.1 Data Acquisition

One color video camera and two color CCD digital cameras are mounted on the ROV, each with a housing cover. The video camera is used to navigate the ROV. The CCD cameras are used to capture the desired objects for measurements which are two Sony ultra-small interline CCD color cameras with an image size of 768 x 494 (picture elements). The sensing area is 6.4mm x 4.8mm. The external synchronization frequency in the vertical direction is 59.94±0.0009Hz, and that in the horizontal direction is 15734.264±0.016Hz. Four electronic shutter speeds are available: 1/60s, 1/50s, 1/100s and 1/1000s. Focal lenses from 3.5mm to 12mm can be chosen. Each camera is housed and covered with a flat front cover lens for waterproof. An artificial illuminating source using two Halogen lamps (USHIO, Japan) is also provided.

2.2.2 Data Transmission

Currently, the tethered transmission mode is applied. The fiber-optic transmission will be a highly recommended option for the future use which supplies a maximum signal quality for real time transmission. The assessment of the degradation of signal quality during the transmission and the effect of signal compression remain as two important topics to be researched.

2.2.3 Data Recording and Retrieving

Two Sony CVD-100 computer controlled Hi-8 video decks are applied to record image sequences from the two CCD cameras, respectively. The exposure time of the two cameras is synchronized and the synchronized time-tags are simultaneously recorded. An image recording and retrieving system, called IOS2-EYE, is implemented. It has utilities especially designed for retrieving the large amount of underwater stereo image sequences, such as image selection for measuring a specific object. Individual digital image pairs can be grabbed during the survey in real-time and can also be converted from the analog images.

2.2.4 Data Control

This control component serves as a center unit. Two monitors are connected to the video camera and CCD cameras. The operator can control the ROV to capture the images of the desired objects, with the help of viewing the color images from the video camera. The ROV can be controlled manually by operating a control panel.

3. UNDERWATER PHOTOGRAMMETRIC MODEL

In underwater photogrammetry, the propagation of the light ray from an object point to its image point is refracted at different media surfaces. Thus, the central perspective imaging geometry does not hold anymore. As shown in Figure 3, the systematic displacement of the ray on the image plane caused by the medium refraction is significant and not negligible. In the following, two models addressing the medium refraction problem are described. A medium refraction correction formula for our imaging system is derived.

3.1 Reduced Central Perspective Model

The objective of this model, called reduced central perspective model, is to compensate the refraction by corrections applied on the image plane so that photogrammetric principles using central perspective geometry can be used. Illustrated in Figure 3, if the correction Δr is obtained ($\Delta r = pp''$), a pseudo central perspective light ray can then be determined. Based on the imaging system, the image correction for the medium refraction is derived.

Let $\Delta r = pp''$ and $r = Cp$. As shown in figure 3, we have

$$\Delta r/r = PP''/P''N = (PP'+P'P'')/P''N$$
$$PP' = p_2p_2' = d\,(\tan\theta_1 - \tan\theta_2)$$
$$P'P'' = H\,(\tan\theta_1 - \tan\theta_3) \qquad (1)$$

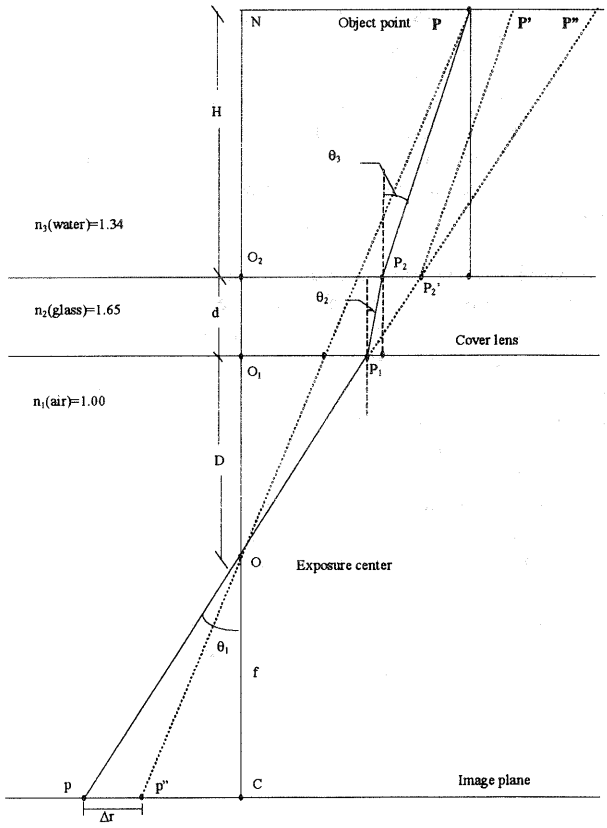

Figure 3. Underwater photogrammetric model

Furthermore, we have

$$P''N = (D+d+H)\tan\theta_1 \quad (2)$$

The correction equation is obtained as

$$\Delta r/r = d\,(1-\tan\theta_2/\tan\theta_1)/(D+d+H) + H\,(1-\tan\theta_3/\tan\theta_1)/(D+d+H) \quad (3)$$

where D and d are system constants. H is related to the object point position.

$$H = OP \times f / Op'' - D - d$$
$$OP = sqrt\,((X-Xo)^2+(Y-Yo)^2+(Z-Zo)^2)$$
$$Op'' \approx sqrt\,(f\times f + r\times r) \quad (4)$$

The incident angle can be determined by

$$\tan\theta_1 = r/f \quad (5)$$

and the angles θ_i and θ_j can be computed using Snell's refraction law:

$$n_i \sin\theta_i = n_j \sin\theta_j \quad (6)$$

Incorporating the above correction into the standard collinear equations, the reduced central perspective model becomes

$$x-\delta x-\Delta x = -U/W$$
$$y-\delta y-\Delta y = -(1/ky)\,V/W \quad (7)$$

where,

$$U = L_1X+L_2Y+L_3Z+L_4$$
$$V = L_5X+L_6Y+L_7Z+L_8$$
$$W = L_9X+L_{10}Y+L_{11}Z+1,$$

and ky is a scale factor of the CCD camera, δx, δy are lens distortion corrections, and Δx, Δy are image corrections for media refraction.

$$\Delta x = x\,(\Delta r/r)$$
$$\Delta y = y\,(\Delta r/r) \quad (8)$$

It should be noted that the unknown H is involved in the above corrections. Thus, an iterative solution of Equations (7) is needed.

3.2 3D Ray Tracing Model

Within an imaging system, a light ray originating from an arbitrary point P in the object space with a given starting propagation direction can be traced through the optical system by successive uses of the law of refraction. Based on characteristics of the light ray propagation, algebraic and trigonometric expressions governing the precise path of a chosen initial ray through the optical system can be used to derive ray tracing equations. By applying these equations one can determine the exact intersecting points on the image plane or indeed on any chosen image surface.

In Figure 3, a light ray originating at a point on the ith surface P_i (X_i, Y_i, Z_i) propagates to P_{i-1} (X_{i-1}, Y_{i-1}, Z_{i-1}) on the (i-1)th surface. Assume that the medium between the two surfaces is homogenous with a refractive index n_i. The length of $\overline{p_{i-1}p_i}$ is represented as an auxiliary quantity ρ_i as

$$\rho_i = \sqrt{(X_i-X_{i-1})^2+(Y_i-Y_{i-1})^2+(Z_i-Z_{i-1})^2} \quad (9)$$

Generally, a light ray between the object point P and image point p will be refracted at every refractive surface. In this case, it is assumed that the coordinates of P and p are given, as well as the refractive surfaces by their implicit functions $F_i = F_i(X_i, Y_i, Z_i)$. Each intersection point P_i is situated on the corresponding refractive surface F_i:

$$F_i(X_i, Y_i, Z_i) = 0 \quad (10)$$

At each refractive point, the law of refraction Equation (6) is applied. In order to trace the ray, it is necessary to find θ_i and θ_i' in terms of the incident ray, the normal vector to the surface and the refracted ray. For θ_i, it can be obtained from (Li, 1995):

$$\cos\theta_i = \alpha_i\lambda_i + \beta_i\mu_i + \gamma_i\nu_i \quad (11)$$

where (α_i, β_i, γ_i) are the directional cosines of the ray from P_{i-1} to P_i and (λ_i, μ_i, ν_i) are the elements of the normal vector of refractive surface F_i at point P_i. (α_i, β_i, γ_i) can be derived from:

$$\begin{pmatrix}\alpha_i\\ \beta_i\\ \gamma_i\end{pmatrix} = \frac{1}{\rho_i}\begin{pmatrix}X_i-X_{i-1}\\ Y_i-Y_{i-1}\\ Z_i-Z_i\end{pmatrix} \quad (12)$$

and (λ_i, μ_i, ν_i) can be expressed as:

$$\begin{pmatrix}\lambda_i\\ \mu_i\\ \nu_i\end{pmatrix} = \left[\left(\frac{\partial F_i}{\partial X_i}\right)^2_{p_i} + \left(\frac{\partial F_i}{\partial Y_i}\right)^2_{p_i} + \left(\frac{\partial F_i}{\partial Z_i}\right)^2_{p_i}\right]^{-\frac{1}{2}} \begin{pmatrix}\left(\frac{\partial F_i}{\partial X_i}\right)_{p_i}\\ \left(\frac{\partial F_i}{\partial Y_i}\right)_{p_i}\\ \left(\frac{\partial F_i}{\partial Z_i}\right)_{p_i}\end{pmatrix} \quad (13)$$

Similarly, as in Equations (11) and (12), θ_i' can be obtained from

$$\cos\theta_i' = \alpha_{i+1}\lambda_{i+1} + \beta_{i+1}\mu_{i+1} + \gamma_{i+1}\nu_{i+1} \quad (14)$$

where (α_{i+1}, β_{i+1}, γ_{i+1}) are the directional cosines of the refracted ray or the incident ray referring to the next refractive surface. Using Equations (12-14), and given that the incident ray, the normal vector and the refracted ray on the same plane, it can be derived that

$$n_{i+1}\begin{pmatrix}\alpha_{i+1}\\ \beta_{i+1}\\ \gamma_{i+1}\end{pmatrix} = n_i\begin{pmatrix}\alpha_i\\ \beta_i\\ \gamma_i\end{pmatrix} - (n_i\cos\theta_i - n_{i+1}\cos\theta_i')\begin{pmatrix}\lambda_i\\ \mu_i\\ \nu_i\end{pmatrix} \quad (15)$$

Thus, the refracted ray can be calculated if the directional cosines of the incident ray, the point of intersection of the incident ray with the surface, and the directional cosines of the normal to the surface at that point are known. In our case, the functions of refractive surfaces are reduced to a simple plane equations.

4. SYSTEM CALIBRATION SCHEME

An efficient calibration scheme for the underwater imaging system is proposed (see Figure 4). The system calibration procedure can be divided into four stages:

(1) Several pairs of images of a calibration control frame are taken in air without the waterproof front cover. Thus the conventional collinear equations with the lens distortion corrections and the CCD pixel scale factor are used to perform the calibration. As a result, the values of pixel scale factor, focal length, lens error distribution parameters and relative orientation parameters are obtained. Also, the errors caused by the electronic sources such as CCD linejittle and image recording (A/D conversion) can be identified in preprocessing.

(2) Mount the front covers and repeat the above operations. In this case, the medium refraction should be considered. Firstly, we apply the medium refraction corrections and employ DLT (Direct Linear Transformation) to solve the approximate values of orientation parameters. And then the 3D ray tracing model is used to achieve the accurate results of the parameters.

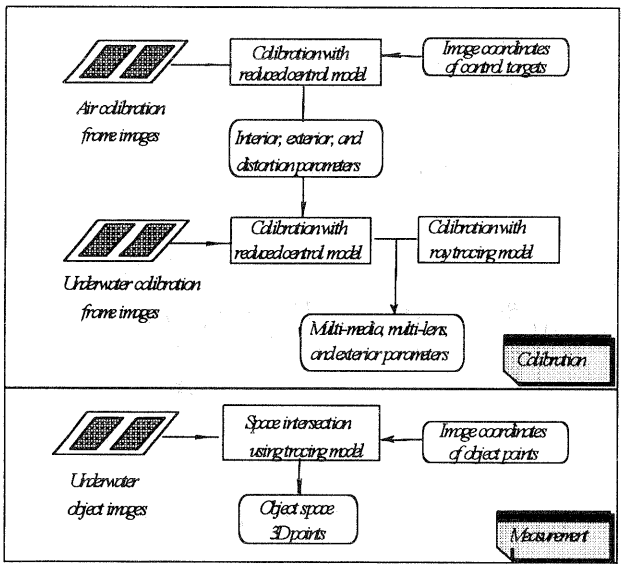

Figure 4. Schematic representation of calibration procedures and object measurement

(3) Place the control frame into the water tank and repeat the above test. The water tank has a cylinder shape with a height and a diameter of about 2.5m.

(4) After the above calibration procedure, the real sea survey can be performed. In a recent test, the imaging system was mounted on a ROV. The stereo image sequences of underwater objects and the control frame on the shallow water seafloor were captured.

5. EXPERIMENTS

5.1 In-air Test With The Front Covers

In the recent test, the baseline of the imaging system was fixed to 400mm and the typical camera-object distance was about 2m. A 1.4×1.4× 0.7m aluminum control frame with 24 control targets was used. Table 1 shows the results of the reduced central perspective model using DLT. In this case, the media indices are treated as 1.0(air) and 1.34(cover). By Comparing the deference of measured camera exterior orientation parameters and computed ones, the computed results are satisfactory. It also demonstrates the derived model is correct. The RMS of adjusted control points (12 control points) are m_x=3.5mm, m_y=3.8mm, m_z=14.9mm, and the final vector RMS is 15.7mm. The accuracy of check points (10 points) are m_x=3.6mm, m_y= 4.0mm, m_z=15.0mm and m_{xyz}=16.1 mm.

Table 1. In-air test with the front covers

Parameter	Left camera	Right camera
f (pixel)	588.61	598.70
x_p (pixel)	275.27	280.62
y_p (pixel)	227.28	213.68
s_y	1.075	1.078
X_0(m)	100.4935	100.8951
Y_0(m)	100.6375	100.6376
Z_0(m)	-97.8093	-97.8027
ω (rads)	-0.0560	-0.0328
ϕ (rads)	-0.0089	0.0084
κ (rads)	-0.0034	-0.0096
$K_1(10^{-2})$	0.00001	-0.00001
$K_2(10^{-6})$	0.00001	0.00010
$P_1(10^{-4})$	-0.01	0.04
$P_2(10^{-4})$	-0.08	0.02

5.2 Real Sea Site Test

A group of stereo pairs of images of the control frame merged in the sea water were obtained. Due to the uncontrolled exterior orientations of the imaging system, the reduced central perspective model using DLT was applied to compute the parameters. The calibration results are shown in Table 2. The computed interior parameters (x_p,y_p,f) are different from the ones in Table 1. The differences may be caused by the correlation existing between the refraction corrections and the lens distortion corrections. These calibrated parameters are employed as approximate values for the 3D ray tracing model. The final results of ray tracing model are that the RMS of control points is m_x=8.4mm, m_y=9.3mm and m_z=2.1mm, respectively. Totally, 13 control points are used for this adjustment. For detail processing of this model, interested readers can find the description in (Li, 1995).

Table 2. Real sea site test

Parameter	Left camera	Right camera
f (pixel)	563.92	569.51
x_p (pixel)	320.02	317.03
y_p (pixel)	223.34	229.71
s_y	1.075	1.078
X_0(m)	101.1556	101.5426
Y_0(m)	100.3727	100.3716
Z_0(m)	-98.1268	-98.3053
ω (rads)	-0.0690	-0.0453
ϕ (rads)	-0.2890	-0.2151
κ (rads)	-0.0624	-0.0131
$K_1(10^{-2})$	-0.0001	-0.0001
$K_2(10^{-6})$	0.00001	0.00001
$P_1(10^{-4})$	-0.006	-0.02
$P_2(10^{-4})$	-0.020	-0.021

6. CONCLUDING REMARKS

The underwater photogrammetric models for extracting quantitative spatial information of underwater objects using CCD stereo images have been researched. In addition, a PC based UDPS has been developed to perform the underwater photogrammetric processing. From the testing results, the following conclusions can be drawn:

- The newly derived reduced central perspective model was successfully applied to compute the calibration parameters of the imaging system. This method provides us an efficient way to address the problems of acquisition of approximate values, especially in uncontrolled underwater environmental situations.
- It is possible to use the 3D optical ray tracing technique to describe the imaging procedure and to construct a rigorous photogrammetric model with multiple refraction and multi-lens of the imaging system.
- The designed system using CCD cameras and mobile photogrammtric method are efficient for underwater data acquisition. It is a promising way to perform a non seafloor control survey.
- The method applied allowed an accuracy of 0.5-1.0 cm along the x- and y-direction and 1.0-3.0 cm along the z-direction in the object space.

The further research will focus on the error and reliability analysis of the imaging system under different underwater conditions. The integration of multiple sensors for objects measurement will be conducted. Digital image classification and pattern recognition for specific objects, e.g., fish species, will be carried out.

7. ACKNOWLEDGMENTS

The support from the Canadian Hydrographic Services (CHS), Department of Fisheries and Oceans (DFO), and the National Sciences and Engineering Research Council of Canada (NSERC) is gratefully acknowledged.

8. REFERENCES

Adams, L. P., 1982. Underwater Analytical Photogrammetriy Using Non-metric Cameras, Int. Archives of Photogrammetry, 25(5):12-22.

Fryer, J. G. and C. S. Fraser, 1986. On the Calibration of Underwater Cameras, Photogrammetric record, 12(67): 73-85

Kotowski, R., 1988. Phototriangulation in Multi-media photogrammetry, Int. Archive of ISPRS, Com. V, Part 27: 324-334.

Leatherdale, J. D. and D. J. Turner, 1991. Operational experience in underwater photogrammetry, ISPRS J. of P&RS, 46, pp. 104-112.

Lenz, R., 1987. Lens Distortion Corrected CCD-camera calibration Points for Real-Time 3D Measurements. Proc. of Inter Commmission on "Fast Processing of Photogrammetric Data", Interlaken, pp. 60-67.

Li, H., 1995. Quantitative Analysis of Underwater Stereo Video Images, M.Sc. Thesis, The University of Calgary.

Rinner, K., 1969. Problems of two medium photogrammetry. PE, 35(2): 275-282

Turner, D. J., D. Yule, and J. Zanre, 1992. A Real Time Photogrammetry System for Underwater and Industrial Applications. Int. Archives of ISPRS, Part 28(5):507-513.

Welham, L. G., 1984. The Development of an Underwater Measuring Capability Using Photogrammetric Technique. Int. Archives of ISPRS, 25(5): 757-766